Water Management
Volume 165 Issue WM1

Local scour due to sediment-carrying free-overfall water jet
Ghodsian, Melville and Coleman

ice | proceedings

Proceedings of the Institution of Civil Engineers
Water Management 165 January 2012 Issue WM1
Pages 21–29 http://dx.doi.org/10.1680/wama.2012.165.1.21
Paper 900009
Received 17/09/2010 Accepted 03/05/2011
Keywords: barrages and reservoirs/dams/river engineering

ice Institution of Civil Engineers publishing

Local scour due to sediment-carrying free-overfall water jet

1 **Masoud Ghodsian** BE, PhD
Professor, Faculty of Civil and Environmental Engineering and Water Engineering Research Institute, Tarbiat Modares University, Tehran, Iran

2 **Bruce Melville** BE, PhD, FRSNZ, DistFIPENZ, MASCE
Professor, Department of Civil and Environmental Engineering, The University of Auckland, New Zealand

3 **Stephen Coleman** BE, PhD, MIPENZ
Associate Professor, Department of Civil and Environmental Engineering, The University of Auckland, New Zealand



Results are presented of 80 experiments on the time variation of scour in uniform bed materials due to a sediment-laden free-overfall jet. It was found that the scour hole characteristics (i.e. the depth of scour, the width of the scour hole, the length of the scour hole and the height of the ridge formed downstream of the scour hole) are functions of the densimetric Froude number, the ratio of drop height to tailwater depth, the ratio of drop height to hydraulic radius of jet, sediment number, and the non-dimensional development time. The influences of different parameters on the longitudinal and lateral profiles of the scoured bed are investigated. Increasing the sediment load in the water jet leads to a decrease in the dimensions of the scour hole. Scour profiles at different times are geometrically similar, and can be expressed by a polynomial using relevant parameters. New empirical equations for the prediction of developing scour-hole geometry and downstream ridge height are presented.

Notation

The following symbols are used in this paper.

B width of tailwater
b_w width of jet
d_{50} median sediment grain size
E average percentage error $= (100/N).\sum_1^N ((computed_i - observed_i)/observed_i)$
Fr_d densimetric Froude number $Fr_d = V/[gd_{50}(S_s - 1)]^{1/2}$
g acceleration due to gravity
H_c drop height measured from the centre of the jet to the bed
h_m sediment ridge height downstream of scour hole
L horizontal distance
L_s length of scour hole
N number of data points
Q outlet flow jet discharge
Q_s sediment mass flow rate in the jet
q unit jet flow discharge
q_s unit volume discharge of sediment in the jet
R jet hydraulic radius
r^2 correlation coefficient
S_s sediment specific gravity
t time of scouring
V exit jet velocity
W width of scour hole
Y vertical distance
Y_s depth of scour hole
Y_t tailwater depth
ρ density of water
ρ_s density of sediment
ϕ scour hole dimensions (including downstream ridge height).

1. Introduction

Flow over and through hydraulic structures often occurs in the form of jets. The jet velocities are usually high enough to produce sizeable, even dangerous, scour holes. The extent of the resulting scour depends on the nature of the bed material and the flow characteristics. The erosion process is quite complex and depends on the interaction of hydraulic and morphological factors.

Several investigators have studied the scour due to a free-overfall jet, including Robinson (1971), Rajaratnam and Beltaos (1977), Rajaratnam (1980), Abt *et al.* (1984), Mason (1989), Mason and Arumugam (1985), Ruff *et al.* (1987), Blaisdell and Anderson (1988), Amanian (1993), Doehring and Abt (1994), Stein and Julien (1994), Azar (1998), Hoffmans (1998), Martins (1999), Ojha (1999), Ghodsian and Azar (2001, 2002), Ghodsian (2002), Najafi (2003), Ghodsian and Najafi (2003), Tajkarimi (2004), Dey and Raikar (2007), Ghodsian *et al.* (2007) and Pagliara *et al.* (2008). Doehring and Abt (1994) and Ojha (1999) studied jet

scour and correlated the dimensions of the scour hole to drop height and $V/\sqrt{gR}$ (V is the velocity, g is the gravitational acceleration and R is the hydraulic radius of jet at the outlet). Ruff *et al.* (1987) and Ghodsian (2002) correlated the dimensions of the scour hole downstream of a culvert to $V/\sqrt{gR}$. Rajaratnam and Beltaos (1977) and Najafi (2003) correlated the depth and width of scour holes due to a vertical jet to densimetric Froude number (defined by Equation 6) and ratio of drop height to jet diameter. Dey and Raikar (2007) correlated the depth of scour hole to densimetric Froude number, ratio of sediment size to jet thickness and ratio of tailwater depth to jet thickness.

All of the previous studies have focused on scour due to a sediment-free water jet. The aim of the present study is to investigate experimentally the influence of a sediment-carrying jet on the dimensions of the scour hole and height of the ridge formed downstream of the scour hole. The temporal development of the scour hole and of the ridge height is addressed. The effects of flow parameters (i.e. discharge and tailwater) on the scour characteristics are also investigated.

2. Dimensional analysis

The scour geometry due to a free-falling jet depends on a range of variables, including velocity of outflow jet V, unit discharge of sediment load in the jet q_s, drop height H_c (measured from the centre of the jet to the bed), cross-sectional dimensions of the jet, density of water ρ, median sediment size d_{50}, density of sediment ρ_s, tailwater depth Y_t, acceleration due to gravity g, width of jet b_w, width of tailwater B and time of scouring t. In this study, the hydraulic radius R (defined in terms of area and wetted perimeter of the jet cross-section at the jet outlet) is used to characterise the jet size. Some investigators have characterised the geometry of the jet by its width for rectangular jets or its diameter for circular jets. Some others have used hydraulic radius. For example, Ruff *et al.* (1987), Doehring and Abt (1994) and Ghodsian (2002) used hydraulic radius for scour due to the outflow jet from a culvert. More recently Ghodsian *et al.* (2007) also used the hydraulic radius for scour due to circular and rectangular outflow jets.

If ϕ represents the dimensions of the scour hole or the ridge height downstream of the scour hole, one can write

$$\phi = f\left(R,\ Y_t,\ d_{50},\ \rho,\ \rho_s,\ g,\ V,\ H_c,\ q_s,\ t,\ b_w,\ B\right) \quad (1)$$

Dimensional analysis of (1) gives

$$\frac{\phi}{Y_t} = f\left(\frac{R}{Y_t}, \frac{d_{50}}{Y_t}, \frac{Y_t g}{V^2}, \frac{H_c}{Y_t}, \frac{q_s}{\sqrt{g Y_t^3}}, \frac{g t^2}{Y_t}, \frac{\rho_s - \rho}{\rho}, \frac{B}{Y_t}, \frac{b_w}{Y_t}\right) \quad (2)$$

The above equation can be written as

$$\frac{\phi}{Y_t} = f\left(\frac{Y_t}{H_c}, \frac{d_{50}}{Y_t}\frac{Y_t g(\rho_s - \rho)}{V^2\rho}, \frac{H_c}{Y_t}\frac{Y_t}{R}, \frac{\rho_s - \rho}{\rho}, \frac{d_{50}}{Y_t}\frac{Y_t}{H_c}, \frac{q_s}{\sqrt{g Y_t^3}}, \frac{V^2}{g Y_t}\frac{g t^2}{Y_t}, \frac{b_w}{B}, \frac{b_w}{H_c}\right) \quad (3)$$

or

$$\frac{\phi}{Y_t} = f\left(\frac{Y_t}{H_c}, Fr_d, \frac{H_c}{R}, \frac{q_s}{\sqrt{g Y_t^3}}, \frac{Vt}{Y_t}, \frac{\rho_s - \rho}{\rho}, \frac{d_{50}}{H_c}, \frac{b_w}{B}, \frac{b_w}{H_c}\right) \quad (4)$$

Based on previous studies (Ghodsian *et al.*, 2007) as well as exploratory data analysis, after combining second and third terms on the right-hand side of the above equation the following dimensionless relationship may be proposed for modelling the phenomenon from Equation 4

$$\frac{\phi}{Y_t} = f\left(\frac{Y_t}{H_c}, Fr_d\frac{R}{H_c}, \frac{q_s}{\sqrt{g Y_t^3}}, \frac{Vt}{Y_t}, \frac{\rho_s - \rho}{\rho}, \frac{d_{50}}{H_c}, \frac{b_w}{B}, \frac{b_w}{H_c}\right) \quad (5)$$

in which Fr_d is the densimetric Froude number given by

$$Fr_d = \frac{V}{\sqrt{g d_{50}(S_s - 1)}} \quad (6)$$

where S_s is specific gravity of the sediment.

In accordance with Equation 5, the following functional relationship is assumed for the different scour parameters. The values of d_{50}/H_c, $(\rho_s - \rho)/\rho$, b_w/H_c and b_w/B were constant in all the experiments and were eliminated from Equation 5.

$$\frac{\phi}{Y_t} = a\left(\frac{Y_t}{H_c}\right)^b\left(Fr_d\frac{R}{H_c}\right)^c\left(\frac{Vt}{Y_t}\right)^d\left(1 - e\frac{q_s}{\sqrt{g Y_t^3}}\right)^f \quad (7)$$

where a, b, c, d, e and f are empirical coefficients or exponents. The second term on the right-hand side of Equation 7 was also used by Tajkarimi (2004) and Ghodsian *et al.* (2007). Rajaratnam

and Beltaos (1977), Ojha (1999) and Najafi (2003) also used this parameter, expressing it in terms of jet diameter D instead of hydraulic radius R. The parameter Vt/Y_t, which represents the temporal evolution of scour, is adopted following the analysis of Dey and Westrich (2003) for an outflow jet from a sluice gate. They used jet thickness instead of tailwater depth. Different forms of equations (incorporating t and q_s) were tested and the one presented (Equation 7) was found to be the best.

3. Experiments

The experiments were conducted in a re-circulating flume with a length of 20 m, width of 0·83 m and depth of 1·0 m. A rectangular free-overfall jet of 0·072 m width was established 5 m from the upstream end of the flume (Figure 1). For this purpose, a channel of length 1·5 m and width of 0·072 m elevated at about 0·26 m from bed level was used to form the jet. The bed of the flume downstream from the jet was raised in order to create a 0·3 m deep and 3 m long test section. The test section was filled with a uniformly-graded sediment with a median diameter $d_{50} = 0{\cdot}62$ mm and standard deviation $\sigma = \sqrt{d_{84}/d_{16}} = 1{\cdot}3$. Here d_{84} and d_{16} are sediment diameters which are finer than 84 and 16% of bed materials, respectively.

A sluice gate was used to control the tailwater depth. Discharge was measured by a calibrated sharp-crested triangular weir at the entrance to the jet approach channel. The depth of flow upstream of the weir and the eroded bed profile were measured using a depth sounder. Initially, a thin protective metal sheet was placed on the sediment bed downstream of the jet. The flume was slowly filled and then water was recirculated. The desired tailwater level was controlled by a sluice gate. The protective sheet was carefully removed so that disturbances of the bed were avoided. The jet-scour experiments were started when the protective sheet was removed. At the end of the experiments, the scour-depth profile was measured using the depth sounder to an accuracy of ±1 mm in the vertical direction.

Initially, experiments were run with a clear-water jet flow and thereafter with a successively-increased sediment load to the jet. Sediment having the same size as that of the bed material ($d_{50} = 0{\cdot}62$ mm) was added to the jet using a hopper (see Figure 1). The hopper was installed at a distance of about 0·10 m upstream from the free overfall. The sediment feed, in the sediment-laden experiments, was started immediately after the protective sheet was removed and was continuous throughout each experiment. The sediment was introduced to the jet such that no deposition took place upstream of the free overfall. The volumetric outflow rate of sediment was measured during each run. Each experiment was started with the known initial volume of sediment in the hopper and after each run the volume of sediment in the hopper was recorded. The difference between the two volumes was considered as the volume of the sediment added to the jet. Experiments were run for varying water and sediment discharges and tailwater conditions. In order to study the time variation of the scour geometry, bed-profile data were recorded. The duration of experimental runs for most of the sediment-laden jet flow experiments was set to 2 h. It was observed that most of the scour had occurred after 2 h (see Figure 2). Therefore, it was decided to limit the duration of sediment-laden jet flow experiments to 2 h. The experimental data are presented in Table 1. In this table, $Q = qb_w$ is the jet discharge, $Q_s = \rho_s q_s b_w$ is the sediment load in the jet, L_s is the length of the scour hole, W_s is the width of scour hole (see Figure 3), Y_s is the depth of scour and h_m is the sediment ridge height.

4. Results

The scour hole is roughly circular in plan (Figure 3), with most of the eroded material being deposited as a ridge downstream from the scour hole. Limited deposition occurs also on the sides of the scour hole. Figure 3 shows that under the stronger flow of $Q = 2{\cdot}97$ l/s, more sediment was transported downstream with deposition on the sides of the scour hole being sparse.

The influence of the tailwater depth Y_t on the longitudinal profile of the scour hole is demonstrated in Figure 4, for a case where

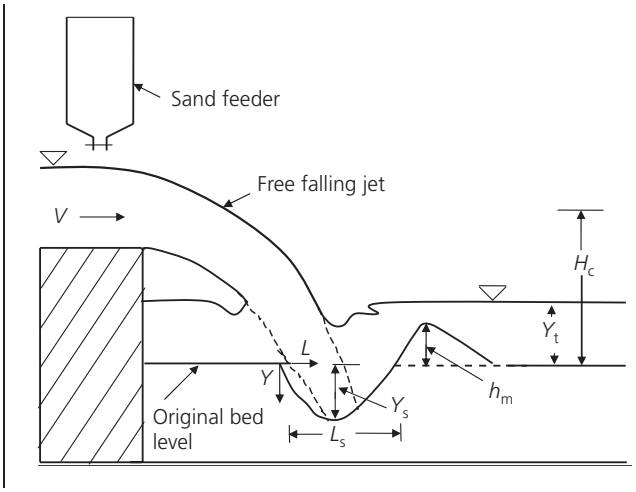

Figure 1. Schematic view of scour due to freefalling jet (not to scale)

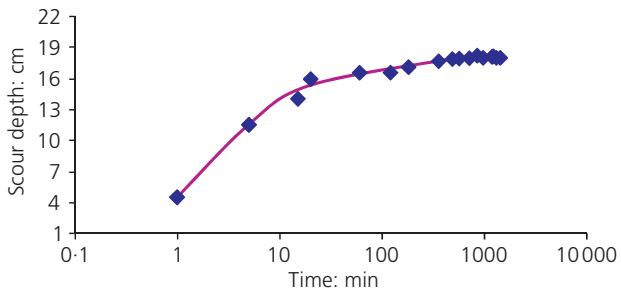

Figure 2. Scour depth versus time for $Q = 3{\cdot}02$ l/s, $Y_t = 15{\cdot}8$ cm and $Q_s = 0$

Q: l/s	Y_t: cm	Time: h	Q_s: g/s	Y_s: cm	L_s: cm	W_s: cm	h_m: cm
0·972	7·7	18·3	0	9·4	42·5	40	5·4
1·592	8·75	18·45	0	9·5	44·15	38·5	5·4
1·592	10·5	4	0	9·85	47	42·5	6·25
1·682	10·5	2	0	10·2	49	47	7
1·682	10·5	2	0	10·24	49	46·5	7·05
1·682	9·07	62·2	0	10·3	50	44	6·1
0·1465	9·55	4	0	10·55	50	42·5	7·8
1·453	9·37	15	0	10·3	47·5	42·5	6·8
1·453	9·37	2·1	0	8·5	50	49	7
1·453	9·37	2	0	9·5	50	49	6·4
1·453	9·37	16	0	8·5	50	49·5	6·1
1·453	9·4	23	0	10·6	49	51	6·6
1·453	9·4	2	0	8·14	43·5	40·5	6·75
1·453	9·4	2	2·295	6·2	37·5	31·5	7
1·453	9·4	2	2·92	4·95	38	31·5	7·75
1·453	9·4	2	3·339	5·3	38·5	29·5	7·65
1·453	11·3	2	0	9·6	45	42·25	7·4
1·453	11·3	2	2·504	5·41	38·5	29·5	6·8
1·453	11·3	2	3·96	4·33	36	24·5	8·05
1·453	11·3	2	4·842	0·7	25	20	9·3
1·453	15·8	2	0	13·7	49	46	9
1·453	19·8	2	0	13·23	53	46·5	7·9
1·453	15·8	2	1·6696	10·7	45	37·5	9·4
1·453	15·8	2	2·9219	5·4	38	53·5	10·5
1·453	15·8	2	5·009	3·3	31	16	10·7
2·9718	9·55	2	0	12·34	53·75	52·5	8
2·9718	9·55	19	0	16·51	68	61	9·4
2·9718	9·55	2	1·878	12·24	56·5	56	7·6
2·9718	9·55	2	3·756	11·7	51·5	49·5	8·1
2·9718	9·55	2	9·6	8·72	46	40·5	8·95
2·9718	15·8	2	0	17·1	64	55	10·7
2·9718	15·8	2	4·382	14·12	60·5	49	11·95
2·9718	15·8	2	7·096	12·65	55·5	48	12·5
2·9718	15·8	2	13·792	6·46	38·5	30	14·8
2·9718	20·3	2	0	15·69	63·5	58	9·35
2·9718	20·3	2	4·591	13·87	57·5	48·5	11·2
2·9718	20·3	2	7·9909	12·33	53	47	12·6
2·9718	20·3	2	13·566	9·36	47	38	14·8
2·9718	11·3	2	0	14·94	60	53	9·2
2·9718	11·3	2	3·965	10·87	50·5	46·5	9·1
2·9718	11·3	2	2·7132	12·81	53	51	9·3
2·9718	11·3	2	6·678	9·92	44·5	43	9·9
3·103	10·5	0·0833	0	9·61	48·5	45	7·4
3·103	10·5	0·0833	4·362	10·82	49	43·5	8·15
3·103	10·5	0·0833	3·233	9·5	48·5	44	8·25
3·103	10·5	0·0833	1·3336	9·24	48	45	7·75
3·103	10·5	0·0833	12·011	10·23	50	*	7·35
3·103	10·5	0·0833	18·559	7·56	46·5	*	8·35
3·103	10·5	0·0833	0	9·4	50	*	7·4
3·103	10·5	0·0833	5·5	8·98	49	*	7·45
3·103	10·5	0·0833	40·44	6·35	79	40	9·15
3·103	10·5	4	0	15·53	60	60·5	1·2

(*continued*)

Q: l/s	Y_t: cm	Time: h	Q_s: g/s	Y_s: cm	L_s: cm	W_s: cm	h_m: cm
3·103	10·5	8·15	0	16·17	60·5	60·5	8·6
3·103	10·5	62·4	0	18·9	65·5	*	8·8
3·103	15·8	8	0	17·77	62	*	8·6
3·103	20·3	8	0	17·58	71	62·5	10·15
3·103	25·6	7		15·69	70	60	10·1
1·5802	9·15	8	0	7·77	43	39	6·4
1·5802	9·55	26·03	0	8·35	43·5	41·5	6·95
1·5802	9·55	4	0	7·4	39	37·5	6
1·5802	9·55	2	0	7·3	51·5	35	6·15
1·5802	9·55	15	0	8·03	42	39	6·6
1·5802	11·4	8	0	8·37	42	40	6·3
1·5802	11·4	15	0	8·98	42·5	41	7·7
1·5802	11·9	2	0	7·78	40·5	38	7·1
1·5802	11·4	4	0	8·29	40·5	40·5	6·1
1·5802	16·4	15	0	14·2	53·5	52	8·5
1·5802	16·4	4	0	13·52	52	50	8·3
1·5802	16·4	2	0	12·96	48	47·5	8·05
1·5802	16·4	22	0	14·85	53·5	56	8·65
1·5802	23·3	19	0	14·22	54·5	49	9·4
3·0239	10·4	24	0	16·47	64	63·5	8·7
3·0239	10·4	15·2	0	14·27	50	59	8·15
3·0239	10·4	4·25	0	12·44	53·5	52	7·95
3·0239	10·4	2	0	11·13	52·5	49	7·8
3·0239	14·5	15·05	0	16·74	67·5	35	10·8
3·0239	15·8	23·5	0	17·47	66·5	64	11·3
3·0239	20·3	23·15	0	16·9	72	*	11·9
3·0239	24·8	24·13	0	16·22	71	58	10·3
3·0239	24·8	24·1	0	16·2	70	58	10·2

* Not measured.

Table 1. Experimental data

$Q = 2{\cdot}97$ l/s and $Q_s = 0$. This figure shows that the dimensions of the scour hole and the ridge height for lower values of Y_t increase with increasing Y_t (i.e. for $Y_t = 9{\cdot}55$, 11·3 and 15·8 cm), but when $Y_t = 20{\cdot}3$ cm the reverse trend occurs. However the effect of Y_t on the point of scour initiation is negligible. It is also evident from Figure 4 that the locations of maximum scour depth and maximum ridge height are influenced by Y_t. With increasing Y_t the locations of the maximum scour depth and the maximum ridge height move downstream. Figures 5 to 7 show the effect of Y_t on Y_s, L_s and $h_{m,}$ respectively. Increasing Y_t leads to the dimensions of the scour hole and the ridge height increasing initially and then decreasing. Ghodsian *et al.* (2007) reported the same trend for clear water jet scour. For low values of Y_t, Y_s and h_m are governed by Y_t and increase with larger Y_t. For low Y_t, the ridge acts as a barrier to the scoured material, which remains in the scour zone so that the extent and depth of scour are limited. With increasing Y_t, the scoured material is transported downstream and deposited over the ridge, which gets higher as a consequence. At the same time, the dimensions of the scour hole increase. The decreasing dimensions of the scour parameters at high values of Y_t are attributed to the increasing dissipation of the energy of the jet flow for this case.

Figure 8 shows normalised scour profiles for the different tests, plotted in terms of L/L_s and Y/Y_s, where L and Y are horizontal and vertical distances, respectively (Figure 1). The data in Figure 8 correspond to $Q = 1{\cdot}45$–$3{\cdot}1$ l/s and $Q_s = 0$–$40{\cdot}4$ g/s. The lower-envelope line in Figure 8 represents Equation 8 and the symbols represent measured values.

$$\frac{Y}{Y_s} = 2{\cdot}477\left(\frac{L}{L_s}\right)^3 + 0{\cdot}423\left(\frac{L}{L_s}\right)^2 - 2{\cdot}9\frac{L}{L_s} \quad (8)$$

The influence of $Q_s > 0$ on the scour geometry is depicted in Figures 9 and 10 for $Q = 2{\cdot}97$ l/s and two values of $Y_t = 11{\cdot}3$ and 20·3 cm, respectively. When $Q_s > 0$, the scouring potential of the

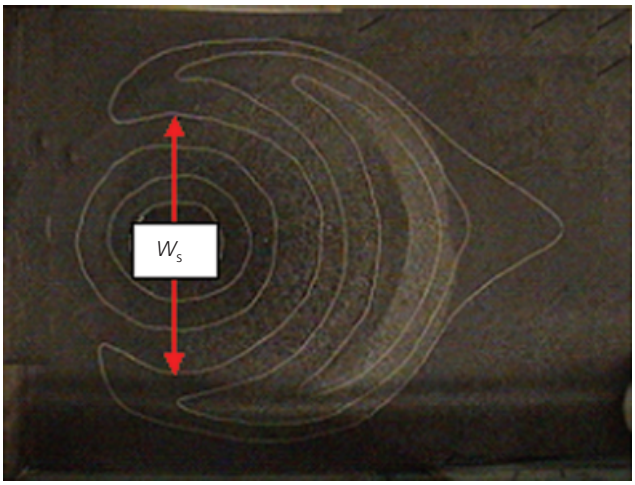

(a)

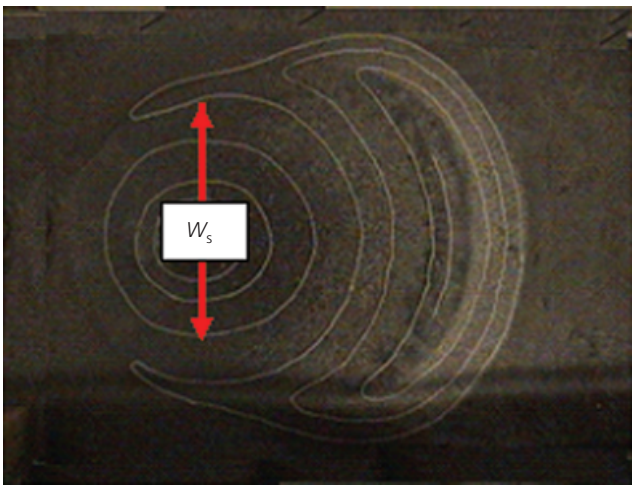

(b)

Figure 3. Typical scour hole formed for two values of discharge with $Y_t = 9{\cdot}5$ cm and $Q_s = 0$: (a) $Q = 1{\cdot}45$ l/s; (b) $Q = 2{\cdot}97$ l/s

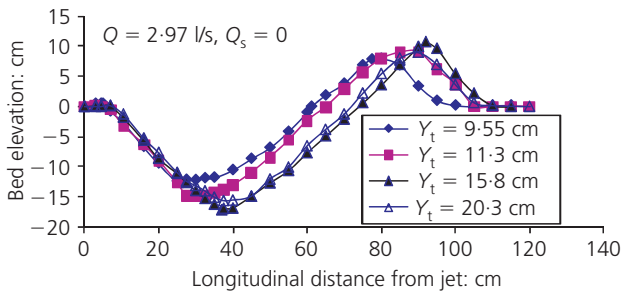

Figure 4. Effect of tailwater depth on scour profile

jet was reduced, and the dimensions of the scour hole decreased (with h_m increasing due to deposition). It is evident that the locations of maximum scour depth, maximum ridge height and the point of scour initiation are not influenced by Q_s. The effect

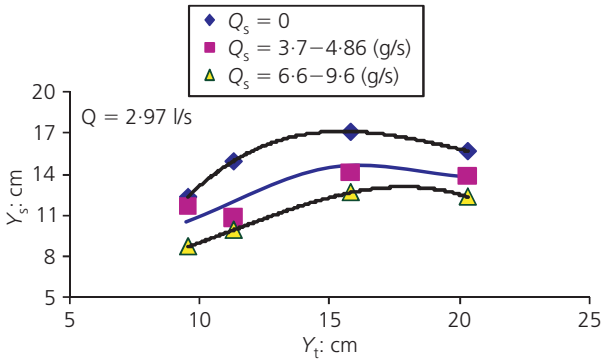

Figure 5. Effect of tailwater depth on depth of scour: $t = 2$ h

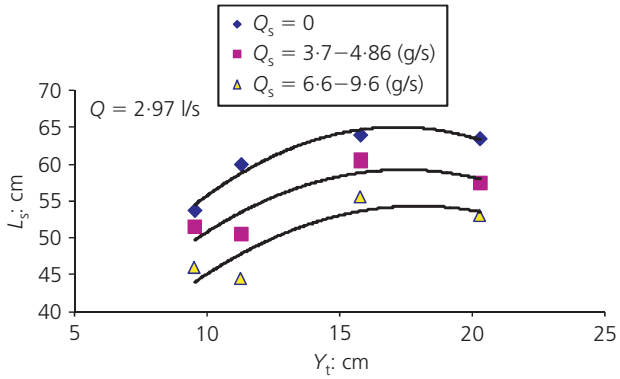

Figure 6. Effect of tailwater depth on length of scour: $t = 2$ h

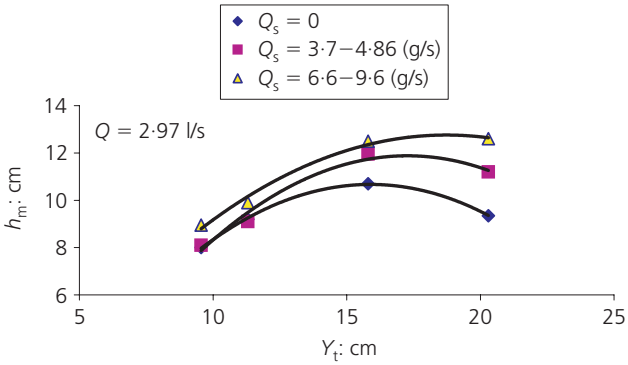

Figure 7. Effect of tailwater depth on height of ridge: $t = 2$ h

of Q_s on the measured values of Y_s and h_m for two values of Y_t is given in Table 2. These effects are also demonstrated in Figures 5 to 7. The trends evident in these figures are similar to those for a clear water jet. Figure 7 shows that at low values of Y_t, the effect of $Q_s > 0$ on h_m is less significant. In this case, Y_t has more influence on h_m and sediment is transported further downstream rather than accumulating on the ridge. At high values of Y_t, h_m is also influenced by the sediment in the jet.

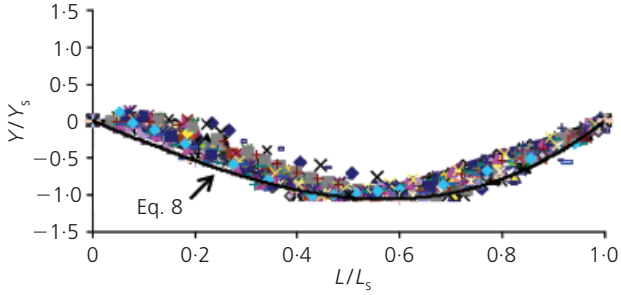

Figure 8. Normalised scour profile for all the present data

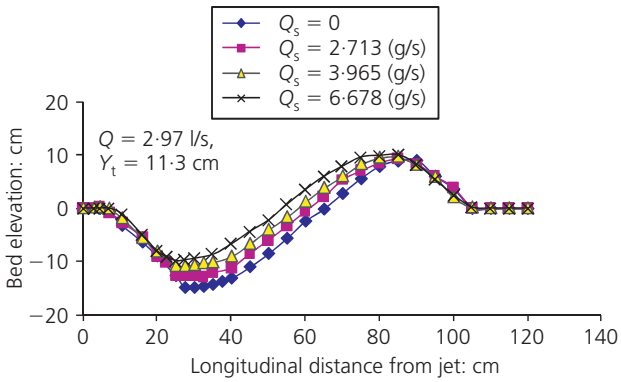

Figure 9. Effect of Q_s on scour profile: $Y_t = 11{\cdot}3$ cm and $t = 2$ h

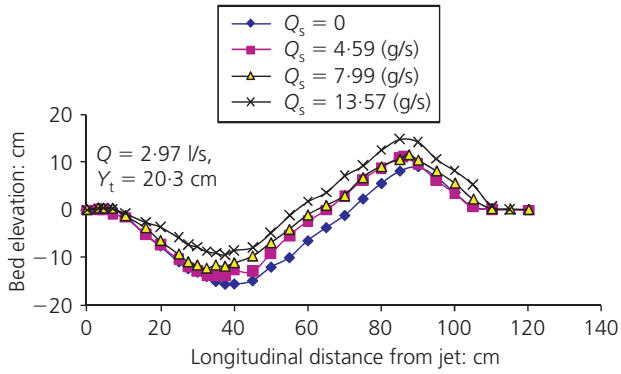

Figure 10. Effect of Q_s on scour profile: $Y_t = 20{\cdot}3$ cm and $t = 2$ h

The influences of sediment number $q_s/\sqrt{gY_t^3}$ and Y_t/H_c on Y_s/Y_t are shown in Figure 11 for $Fr_dR/H_c = 0{\cdot}65$. Scour depth is seen to reduce with increasing $q_s/\sqrt{gY_t^3}$ and Y_t/H_c. Figure 12 shows the influence of the parameters $q_s/\sqrt{gY_t^3}$ and Y_t/H_c on L_s/Y_t for $Fr_dR/H_c = 0{\cdot}65$. Again, the effect of $q_s/\sqrt{gY_t^3}$ in reducing scour size is clear. The influences of the parameters $q_s/\sqrt{gY_t^3}$ and Y_t/H_c on W_s/Y_t and h_m/Y_t are shown in Figures 13 and 14, respectively, for $Fr_dR/H_c = 0{\cdot}65$. The influence of $q_s/\sqrt{gY_t^3}$ on W_s is similar to that for Y_s and L_s. The influence of Y_t on h_m, as shown in Figure 14, supports the observation above that Y_t governs h_m for shallower Y_t.

For the experimental data at all times (including data for both clear water and sediment-laden conditions), the values of coeffi-

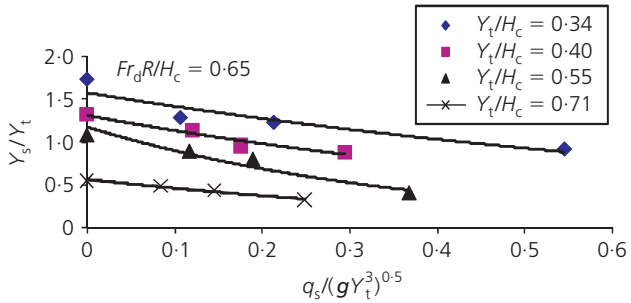

Figure 11. Variations of Y_s/Y_t with $q_s/\sqrt{gY_t^3}$ for different values of Y_t/H_c: $t = 2$ h

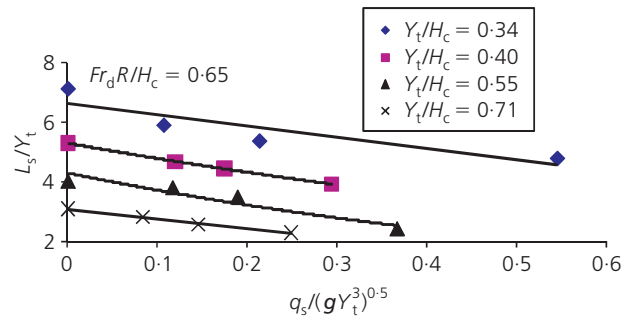

Figure 12. Variations of L_s/Y_t with $q_s/\sqrt{gY_t^3}$ for different values of Y_t/H_c: $t = 2$ h

$Y_t = 11{\cdot}3$ cm			$Y_t = 20{\cdot}3$ cm		
Q_s: g/s	Y_s: cm	h_m: cm	Q_s: g/s	Y_s: cm	h_m: cm
0	15·0	9·1	0	15·7	9·0
2·7	12·8	9·3	4·6	13·8	11·0
3·96	10·9	9·7	8·0	12·3	11·5
6·68	9·9	10·0	13·6	9·4	14·8

Table 2. Effect of Q_s on Y_s and h_m for Q = 2·97 l/s

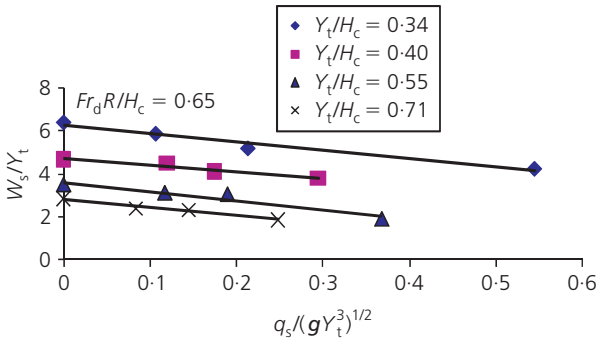

Figure 13. Variations of W_s/Y_t with $q_s/\sqrt{gY_t^3}$ for different values of Y_t/H_c: $t = 2$ h

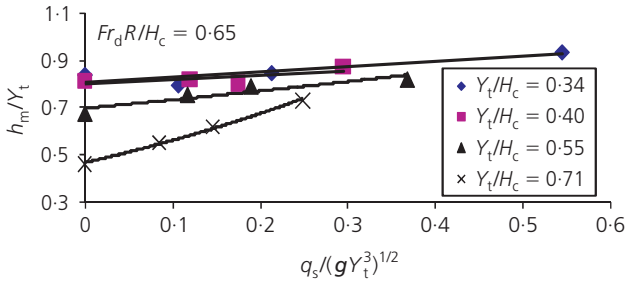

Figure 14. Variations of h_m/Y_t with $q_s/\sqrt{gY_t^3}$ for different values of Y_t/H_c: $t = 2$ h

cients and exponents in Equation 7 are given in Table 3 for Y_s, W_s, L_s and h_m. The correlation coefficient r^2 and the average percentage error E for each case are also given in this table.

Figure 15 presents a typical variation of Y_s/Y_t with V_t/Y_t for $Q = 3l/s$, $Q_s = 0$ and $Y_t = 15{\cdot}8$ cm. Equation 7 adequately predicts the variation of scour depth with time for ranges of $1{\cdot}5 * 10^5 < Vt/Y_t < 5{\cdot}5 * 10^5$, $0{\cdot}29 < Y_t/H_c < 0{\cdot}9$ and $0 < q_s/\sqrt{gY_t^3} < 0{\cdot}6$. The proposed model does not agree well during the early stages of scour and further research is required in order to develop a general equation. Moreover it was found that $q_s/\sqrt{gY_t^3}$ is the most significant parameter affecting the scour depth, with V_t/Y_t having the least effect on scour depth.

5. Conclusions

The conclusions from this experimental study are listed here.

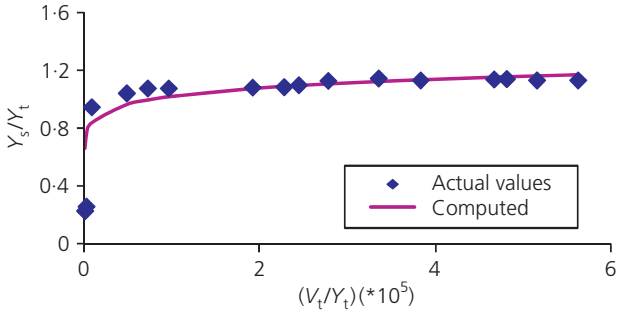

Figure 15. Variation of Y_s/Y_t with V_t/Y_t: $Q = 3$ l/s, $Q_s = 0$ and $Y_t = 15{\cdot}8$ cm

(*a*) The sediment carried by a free-overfall jet reduces the scouring potential of the jet as compared to a clear-water jet, and its effect is included in a new relationship for scour depth estimation.

(*b*) The height of the ridge downstream of the scour hole is influenced by Y_t and Q_s. The influence of Q_s on h_m is less significant at low values of Y_t.

(*c*) With increasing Y_t, the dimensions of the scour hole (Y_s, L_s and W_s) and the ridge height (h_m) initially increase, reach a maximum value and thereafter decrease. This trend is the same for clear water jets and sediment-carrying water jets.

(*d*) The height of the ridge formed at the sides of the scour hole is reduced with increasing discharge.

(*e*) Scour profiles are geometrically similar throughout the development of the scour hole.

(*f*) Equation 7 adequately predicts the time dependency of the scour hole geometry and the height of the downstream ridge for a uniform sediment bed subject to free-overfall water jets of varying relative sediment load.

(*g*) Additional work remains to confirm the presented experiments for varying sediment sizes.

REFERENCES

Abt SR, Kloberdanz RL and Mendoza C (1984) Unified culvert scour determination. *Journal of Hydraulic Engineering ASCE* **110(10)**: 1363–1367.

Amanian N (1993) *Scour Below a Flip Bucket Spillway.* PhD dissertation, Civil and Environmental Engineering, Utah State University, Logan, UT, USA.

Azar FA (1998) *Effect of Sediment Size Distribution on Scour*

Scour parameters	*a*	*b*	*c*	*d*	*e*	*f*	r^2	*E*: %
Depth of scour (Y_s)	1·03	−0·6	0·91	0·09	0·124	1·34	0·73	11·3
Length of scour (L_s)	2·48	−0·82	0·21	0·04	−0·166	2·5	0·72	11·2
Width of scour (W_s)	1·77	−0·94	0·06	0·04	0·378	0·47	0·6	16·2
Height of ridge (h_m)	0·47	−0·42	0·03	0·02	−0·32	0·25	0·52	18·9

Table 3. Values of coefficient and exponents in Equation 7

Downstream of Free Over Fall Spillway. MS thesis, Tarbiat Modares University, Tehran, Iran.

Blaisdell FW and Anderson CL (1988) A comprehensive generalized study of scour at cantilevered pipe outlets. *Journal of Hydraulic Research IAHR* **26(4)**: 357–376.

Dey S and Raikar R (2007) Scour below a high vertical drop. *Journal of Hydraulic Engineering ASCE* **133(5)**: 564–568.

Dey S and Westrich B (2003) Hydraulics of submerged jet subject to change in cohesive bed geometry. *Journal of Hydraulic Engineering ASCE* **129(1)**: 44–52.

Doehring F and Abt SR (1994) Drop height influence on outlet scour. *Journal of Hydraulic Engineering ASCE* **120(2)**: 1470–1476.

Ghodsian M (2002) Scour hole geometry downstream of a culvert. *Proceedings of 13th-IAHR-APD Congress, National University of Singapore, Singapore*, vol. 1, pp. 272–275.

Ghodsian M and Azar FA (2001) Effect of sediment gradation on scour below free over fall spillway. *Proceedings of the 3rd International Symposium on Environmental Hydraulics, ASCE, Arizona State University, USA*, on CD-ROM.

Ghodsian M and Azar FA (2002) Scour hole characteristics below free over fall spillway. *International Journal of Sediment Research* **17(4)**: 304–313.

Ghodsian M and Najafi J (2003) Maximum depth of scour by impinging circular turbulent jet. *Proceedings of the 30th IAHR Congress, Thessaloniki, Greece*, vol. 2, pp. 353–359.

Ghodsian M, Melville B and Tajkarimi D (2007) Local scour due to free over fall jet, *Proceedings of the Institution of Civil Engineers, Water Management* **159(WM4)**: 253–260.

Hoffmans GJCM (1998) Jet scour in equilibrium phase. *Journal of Hydraulic Engineering ASCE* **124(4)**: 430–437.

Martins KJ (1999) *Scour Caused by Rectangular Impinging Jets*. PhD thesis, Colorado State University, Fourth Collins, CO, USA.

Mason PJ (1989) Effects of air entrainments on plunge pool scour. *Journal of Hydraulic Engineering ASCE* **115(3)**: 385–399.

Mason PJ and Arumugam K (1985) Free jet scour below dams and flip buckets. *Journal of Hydraulic Engineering ASCE* **111(2)**: 220–235.

Najafi J (2003) *Scour Downstream of Pipe Culvert*. MS thesis, Tarbiat Modares University, Tehran, Iran.

Ojha CSP (1999) Outlet scour modelling for drop height influence. *Journal of Hydraulic Engineering ASCE* **125(1)**: 83–85.

Pagliara S, Amidei M and Hager WH (2008) Hydraulics of 3D plunge pool scour. *Journal of Hydraulic Engineering ASCE* **134(9)**: 1275–1284.

Rajaratnam N (1980) Erosion by plane turbulent jet. *Journal of Hydraulic Research IAHR* **19(4)**: 339–358.

Rajaratnam N and Beltaos S (1977) Erosion by impinging circular turbulent jets. *Journal of Hydraulic Engineering ASCE* **103(10)**: 1191–1205.

Robinson AR (1971) Model study of scour from cantilevered outlets. *Transaction ASAE* **14(3)**: 571–581.

Ruff JF, Abt SR, Doehring FK and Donnell CA (1987) Influence of culvert shape on outlet scour. *Journal of Hydraulic Engineering ASCE* **113(3)**: 393–400.

Stein OR and Julien PY (1994) Sediment concentration below free overfall. *Journal of Hydraulic Engineering ASCE* **120(9)**: 1043–1059.

Tajkarimi D (2004) *Analysis of Scour due to Free Falling Jet and Application of Neural Network*. MS thesis, Tarbiat Modares University, Tehran, Iran.